CHAPTER 6

STELLAR DYNAMOS

Steven Tobias & Nigel Weiss

6.1. STELLAR MAGNETIC ACTIVITY

Stars that are magnetically active owe this activity to a combination of turbulent convection and rotation. In this review we shall focus on stars like the Sun, which lie on the main sequence and are sufficiently cool that hydrogen becomes ionised below their surfaces, resulting in the presence of a deep outer convection zone. Their magnetic fields can be measured directly through the Zeeman broadening of spectral lines, or inferred from proxy evidence. This is provided by coronal X–ray emission, by H and K emission from singly ionised Ca^+, by photometric variability (associated with starspots) or by optical and radio flares – all of which are known to be associated with magnetic activity on the Sun (Tayler, 1997). The Sun is unique, however, in that we can observe detailed magnetic structures on its surface, and we have records of its activity extending back through many centuries; its internal structure is also well-established (see Figure 6.1). On the other hand, the Sun is a single star whose large-scale properties evolve extremely slowly. So it is only through exploiting the solar-stellar connection and examining the magnetic properties of other stars that we can understand how magnetic activity depends on such key parameters as rotation (Wilson, 1994; Mestel, 1999; Schrijver & Zwaan, 2000).

Chromospheric Ca^+ emission has been measured for a large number of nearby stars, revealing a wide range of activity (Vaughan & Preston, 1980; Soderblom, 1985; Henry *et al.*, 1996). Comparison of middle-aged stars like the Sun with similar stars in young clusters shows that magnetic activity declines with age. Moreover, there

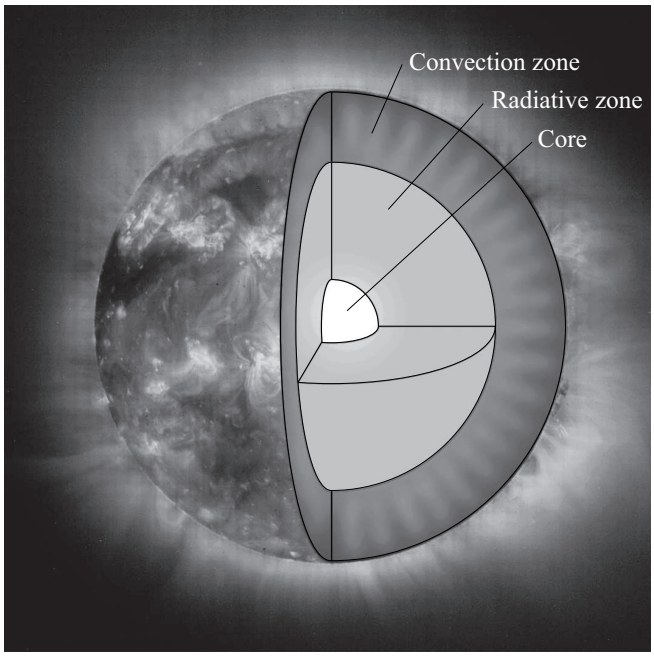

Figure 6.1 - Internal structure of the Sun. The cutaway image shows the visible surface (the photosphere, with a radius $R_\odot \approx 700\,\mathrm{Mm}$), together with an outer region where energy is carried mainly by convection, and an inner region where energy is transported by radiation. The narrow interface between the convection zone and the radiative zone, at a radius of approximately $0.7R_\odot$, has a thickness of only $0.02R_\odot$ and is the site of the tachocline, where there is a strong radial gradient in angular velocity. The temperature rises from $6000\,\mathrm{K}$ at the surface to about $2 \times 10^6\,\mathrm{K}$ at the base of the convection zone and then to $1.5 \times 10^7\,\mathrm{K}$ in the central core, where energy is generated by thermonuclear fusion. (**See colour insert**.)

is a strong correlation between activity and rotation (Noyes *et al.*, 1984; Baliunas & Vaughan, 1985; Saar & Brandenburg, 1999). When stars first arrive on the main sequence and begin to burn hydrogen they are spinning rapidly (Soderblom, Jones & Fischer, 2001), with rotation periods of order a day, but they gradually lose angular momentum to magnetic braking owing (Mestel, 1999) and spin down. It is only in slowly rotating middle-aged stars like the Sun (with rotation periods of order a month) that cyclic activity is found (Baliunas *et al.*, 1995). The cycle periods are all around 10 years: Figure 6.2 shows the time-dependent Ca^+ emission in a solar-type star, exhibiting cyclic variation with a period of 8.2 yr.

The Sun's own magnetic activity varies cyclically, with an average period of about 11 years (Stix, 2002). The most dramatic manifestation of this activity is in sunspots, which are dark because they are the sites of strong magnetic fields that locally inhibit

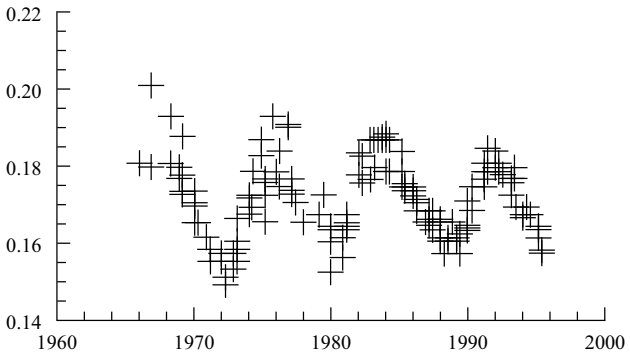

Figure 6.2 - Cyclic activity in a star. Chromospheric Ca^+ emission as a function of time for the K0 star HD 81809 (Mount Wilson Observatory H-K Project).

convection. The cyclic variation of the incidence of sunspots is demonstrated by the well-known butterfly diagram in Figure 6.3. Spots typically appear in pairs with opposite polarity, oriented nearly parallel to the equator. The spots are contained within active regions, which are formed by the emergence of almost azimuthal (or toroidal) magnetic flux, whose orientation obeys Hale's laws. The polarities of leading and following spots are consistent in each hemisphere but antisymmetric about the equator; and these polarities reverse from one activity cycle to the next. Hence the *magnetic* cycle has a period of 22 years. The axis of a sunspot group or active region is actually inclined at a small angle so that leading spots are closer to the equator, and this angle increases systematically with latitude (Joy's law). This result, with the large horizontal scale of active regions, suggests that the emerging flux is deep-seated and not a merely superficial phenomenon.

The arguments for ascribing the origin of these magnetic fields to a dynamo are different from those for planetary dynamos. Whereas the Earth's magnetic field has to be maintained by a geodynamo, since it has been present for billions of years despite an Ohmic decay time of only 10^4 yr, the solar problem is to explain how the field reverses every 11 years when the decay time is 10^9–10^{10} yr. It has been claimed that cyclic behaviour could be driven by an oscillator, with a steady poloidal field and alternating shears in differential rotation, though no mechanism for producing such shears has been suggested. In fact, the Sun possesses a large-scale poloidal field that is most prominent in polar regions and has dipole symmetry, and this field reverses near sunspot maximum (i.e. 90° out of phase with the activity cycle). Furthermore, the only observed fluctuations in angular velocity have a period of 11 years, not 22 years, and an 11-yr periodicity is precisely what is expected from a nonlinear dynamo, since the Lorentz force is quadratic in the magnetic field. We may therefore assume that this cyclic solar activity is maintained by a large-scale homogeneous dynamo, which generates systematic fields (magnetic *climate*) as opposed to the

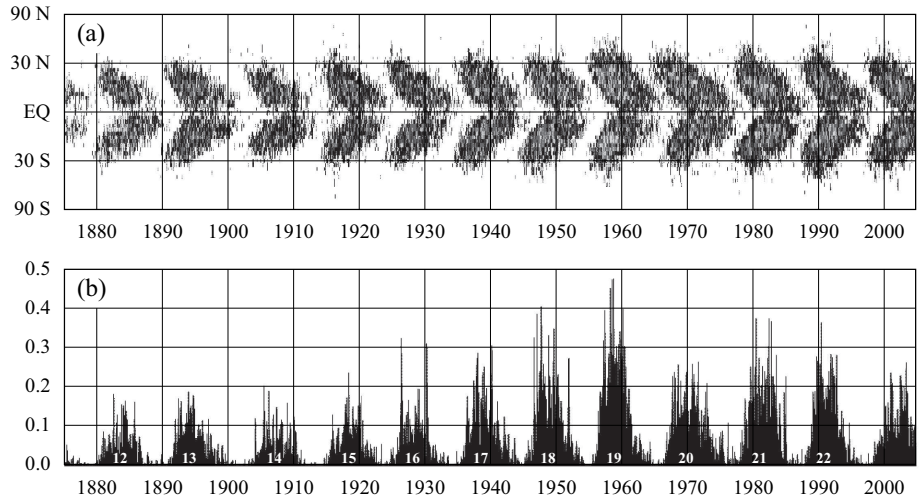

Figure 6.3 - Cyclic activity in the Sun (1874–2004). (a) butterfly diagram, showing the incidence of sunspots as a function of latitude and time; new spots appear at $\pm 30^\circ$ as the old cycle dies away at the equator. (b) area covered by sunspots as a function of time (courtesy of D.H. Hathaway).

small-scale disordered fields (magnetic *weather*) which could be produced by local dynamo action near the photosphere.

The current state of solar dynamo theory forces most of our discussion to be physical rather than mathematical, backed up by numerical rather than by analytical results. In the next two sections we introduce mean field ($\alpha\omega$) dynamos for the solar cycle. Then, in Section 6.4, we focus on dynamos located at the interface between the convective and radiative zones, where the radial shear is greatest. Long-term modulation of cyclic activity is the subject of Section 6.5. Next, in Section 6.6, we consider the enhanced activity in rapidly rotating stars and go on to comment briefly on dynamos in protostellar accretion discs. Finally, we summarise future prospects for stellar dynamo theory. Many of these issues have already been discussed in various recent reviews (e.g. Stix, 1991; Weiss, 1994; Rosner, 2000; Tobias, 2002a; Choudhuri, 2003; Ossendrijver, 2003, Rüdiger & Arlt, 2003).

6.2. LINEAR $\alpha\omega$–DYNAMOS FOR THE SOLAR CYCLE

A proper treatment of the solar dynamo would require an accurate simulation of the nonlinear interactions between rotation, convection and magnetic fields. Direct

numerical simulation of these processes in a regime where the magnetic Reynolds number $\mathrm{Rm} \approx 10^9$ remains beyond the capacity of the largest computers and, in any case, the key physical mechanisms of differential rotation, helicity and magnetic buoyancy are not adequately understood. Apart from some early brave attempts (Gilman, 1983; Glatzmaier, 1985), stellar dynamo theory has had to rely on the mean field approximation (discussed in Section 1.5).

Since differential rotation is so effective at creating toroidal fields, nearly all stellar models are axisymmetric $\alpha\omega$–dynamos. Then the poloidal field $\mathbf{B}_P = \boldsymbol{\nabla} \times (A\mathbf{e}_\phi)$ and the toroidal field $\mathbf{B}_T = B_\phi \mathbf{e}_\phi$ satisfy the linear equations

$$\partial_t A = \alpha B_\phi + \eta \mathcal{D}^2 A \,, \qquad \partial_t B_\phi = r \sin\theta \, \mathbf{B}_P \cdot \boldsymbol{\nabla}\omega + \eta \mathcal{D}^2 B_\phi \,, \tag{6.1a,b}$$

referred to spherical polar co-ordinates, where ω is the local angular velocity, η here denotes the total (laminar plus turbulent) diffusivity and $\mathcal{D}^2 = \Delta - 1/r^2 \sin^2\theta$.

6.2.1. DYNAMO WAVES

Parker (1955, 1979) provided the simplest (and earliest) example of a mean field dynamo. He considered a Cartesian model with $A, \ B \propto \exp(\mathrm{i}\, k\, x)$, where the x–direction corresponds to increasing θ and $U(z)$ represents the sheared zonal velocity with z corresponding to a local radial co-ordinate. He showed that there was exponential growth when the dynamo number (see Section 1.5.3), $\mathrm{D} = \alpha U'/(2\eta^2 k^3)$, was greater in magnitude than unity (prime is used to note a derivative, i.e. $U' = \mathrm{d}U(z)/\mathrm{d}z$). The waves travel "equatorward" if $\mathrm{D} < 0$. This result from a relatively simple model has had a profound effect on stellar dynamo theory; it is now widely claimed that dynamo waves always travel poleward if $\mathrm{D} > 0$. However this is not always the case (although often true) and some solar dynamo models *are* able to reproduce equator-propagating magnetic fields even for $\mathrm{D} > 0$. This result can readily be extended to other geometries and, more generally, the waves travel along surfaces of constant ω.

It is important to realise that the local behaviour of travelling waves with periodic boundary conditions may differ qualitatively from the global behaviour of solutions that are spatially confined, whether in Cartesian or in spherical geometry. For linear theory, this corresponds to the difference between convective and absolute instability (Tobias *et al.*, 1998b). For waves of frequency ω and wavenumber k, governed by the dispersion relation

$$\omega(k; \mathrm{D}) \equiv 0 \,, \tag{6.2}$$

instability in an infinite (or periodic) domain occurs at the smallest value of D that satisfies the dispersion relation for some real k. It is possible therefore to generate a marginal curve of $\mathrm{D}_{\mathrm{crit}}$ versus k (Worledge *et al.*, 1997). In a finite domain of length

Table IV - Some orders of magnitude for the solar dynamo.

Solar radius	$R_\odot$	6.96×10^8	m
Solar mass	$M_\odot$	1.99×10^{30}	kg
Surface temperature		5780	K
Central temperature		15.6×10^6	K
Surface density		2.0×10^{-4}	$\mathrm{kg\,m^{-3}}$
Central density		1.5×10^5	$\mathrm{kg\,m^{-3}}$
Solar age		4.57×10^9	yr
Large scale magnetic field strength		5×10^4	nT $(0.5\,\mathrm{G})$
Diameter of surface granulation	L	10^6	m
Sunspot magnetic field strength		0.3	T $(3000\,\mathrm{G})$
Rotation time at equator		25	d
Rotation time at 60^o latitude		29	d
Ekman number, base of the c.z.	E	$\nu/\Omega R_\odot^2$	$\mathcal{O}(10^{-15})$
photosphere			$\mathcal{O}(10^{-17})$
Rossby number, base of the c.z.	Ro	$\lvert\mathbf{u}\rvert/\Omega R_\odot$	$\mathcal{O}(10^{-2})$
photosphere		$\lvert\mathbf{u}\rvert/\Omega L$	$\mathcal{O}(10^3)$
Prandtl number, base of the c.z.	Pr	ν/κ	$\mathcal{O}(10^{-6})$
photosphere			$\mathcal{O}(10^{-13})$
Magnetic Prandtl number, base of the c.z.	Pm	ν/η	$\mathcal{O}(10^{-1})$
photosphere			$\mathcal{O}(10^{-7})$
Reynolds number, base of the c.z.	Re	$\lvert\mathbf{u}\rvert R_\odot/\nu$	$\mathcal{O}(10^{13})$
photosphere		$\lvert\mathbf{u}\rvert L/\nu$	$\mathcal{O}(10^{13})$
Magnetic Reynolds number, base of the c.z.	Rm	$\lvert\mathbf{u}\rvert R_\odot/\eta$	$\mathcal{O}(10^{11})$
photosphere		$\lvert\mathbf{u}\rvert L/\eta$	$\mathcal{O}(10^6)$

L, instability of a global mode is governed by a more stringent condition. In the limit $L \to \infty$, this condition approaches that for absolute instability of a periodic wavetrain; that is both (6.2) and the condition $\partial\omega/\partial k = 0$ must be satisfied simultaneously. This can only be achieved if k is allowed to be complex (see Kuzanyan & Sokoloff, 1995). It has its origins in the development of the Maximally–Efficient–Generation Approach (MEGA, see Ruzmaikin *et al.*, 1990), as explained in detail in the Appendix of Bassom *et al.* (2005). The two criteria for periodic and finite domains yield very different critical dynamo numbers and frequencies. Moreover, nonlinear behaviour can be qualitatively affected (Tobias 1998), with the frequency in the nonlinear regime being determined by the interaction of the global mode with the boundaries, and the possible presence of secondary absolute instabilities.

6.2.2. SPHERICAL MODELS

The spherical problem possesses two important symmetries with respect to reflection about the equator. The governing equations (6.1a,b), with appropriate boundary conditions and suitable constraints on α and ω, are invariant under the transformations

$$d: \ (\theta, t) \to (\pi - \theta, t), \ \ (A, B) \to (A, -B) \tag{6.3a}$$

and

$$q: \ (\theta, t) \to (\pi - \theta, t), \ \ (A, B) \to (-A, B)\,. \tag{6.3b}$$

These symmetries generate an abelian group (D_2) with four elements, including $i = dq: \ \ (\theta, t) \to (\theta, t), \ \ (A, B) \to (-A, -B)$ and the identity (Jennings & Weiss, 1991). The trivial solution $A = B = 0$ possesses the full D_2 symmetry, which is broken at the initial Hopf or pitchfork bifurcation. The linear problem then allows two distinct families of eigenfunctions, with different symmetries about the equator. For *dipole* solutions, with the symmetry d, the toroidal field B is antisymmetric about the equator, while A is symmetric; for *quadrupole* solutions, with the symmetry q, A is antisymmetric and B is symmetric. If an appropriate dynamo number is defined by setting $\mathrm{D} = \alpha\omega' R_\odot^4/\eta^2$, where $R_\odot$ is the solar radius, then the critical values of D at which dipolar and quadrupolar modes become unstable differ only slightly. Provided that $\mathrm{D} < 0$ in the northern hemisphere, oscillatory dipole modes are marginally favoured and the pattern drifts equatorward. Thus it is easy to construct butterfly diagrams that are qualitatively similar to that in Figure 6.3 (Steenbeck & Krause, 1969; Stix, 1976, 2002). Note that the symmetry of one or other of these solutions can only be broken at a subsequent bifurcation in the nonlinear domain. If this happens at a pitchfork bifurcation, further symmetries of periodic solutions can be classified (Jennings & Weiss, 1991) but symmetry–breaking more commonly involves a Hopf bifurcation that leads to quasiperiodic behaviour.

6.2.3. THE ω–EFFECT

It has long been known that the angular velocity varies with latitude at the surface of the Sun: the equatorial regions rotate distinctly more rapidly (with a sidereal period of 25 days) than the poles (with a period of about 35 days). More recently, one of the triumphs of helioseismology has been the determination of the Sun's internal rotation (Thompson *et al.*, 2003). Measurements of p–mode frequencies have revealed that there is very little radial shear in the convection zone, where $\omega \approx \omega(\theta)$, while ω is nearly uniform in the radiative interior. Between the two is a thin layer (with thickness around $0.02R_\odot$) with a very strong radial shear, the *tachocline*. This observed pattern of differential rotation is displayed in Figure 6.4; since the radiative core rotates at an intermediate rate, $\partial\omega/\partial r$ changes sign at a latitude around 30°.

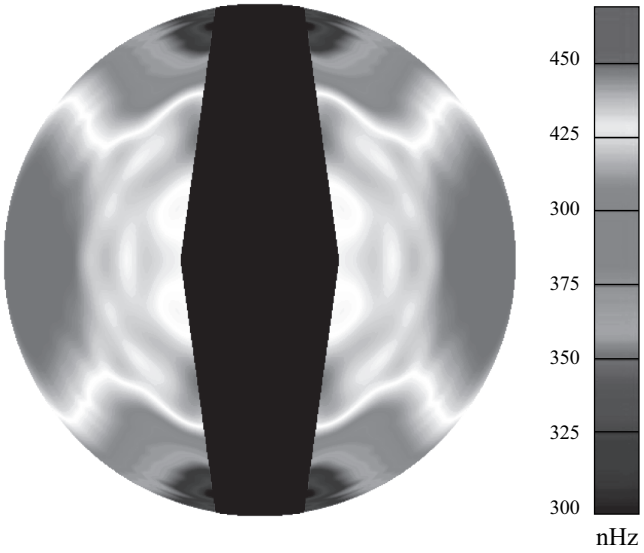

Figure 6.4 - Differential rotation in the solar interior. The rotation rate is approximately constant along radii in the convection zone, whose base is indicated by the dashed line. A frequency of 450 nHz corresponds to a period of about 26 days (courtesy of J. Christensen-Dalsgaard). (**See colour insert**.)

The dynamics within the tachocline is not yet understood (Tobias, 2004) but it is generally accepted that strong toroidal fields are generated and stored within this region of shear.

6.2.4. THE α–EFFECT

The source of the α–effect is much less clear. The earliest treatments assumed that poloidal fields were regenerated by cyclonic eddies that were distributed throughout the convection zone and that α (which is antisymmetric about the equator) reverses its sign in such a way that $\mathrm{D} < 0$ at the base of the convection zone in the northern hemisphere (Parker, 1979; Krause & Rädler, 1980). Some recent authors have revived a surface flux-transport model due originally to Babcock (1961) and to Leighton (1967), in which the α–effect is ascribed to the decay, through turbulent diffusion, of active regions whose orientation is determined by Joy's law. The opposing fields of leading spots cancel out as they approach the equator, while the trailing fields of following spots spread polewards and eventually reverse the polar fields at sunspot maximum. In that case, the amplitude of the activity cycle should determine the strength of the high-latitude poloidal field at the next sunspot minimum. This can be checked by studying the incidence of recurrent geomagnetic

activity, caused by high-speed streams emerging from coronal holes. Detailed investigations show that the toroidal fields at sunspot maximum are more closely related to the mid-latitude poloidal fields that *precede* them than to those that follow afterwards (Simon & Legrand 1986; Hathaway, Wilson & Reichmann 1999; Ruzmaikin & Feynman 2001). This evidence implies that flux transport is only a superficial process.

The dynamo is obviously more efficient if the α–effect is located near the base of the convection zone, where the ω–effect is strong. Indeed, Mason, Hughes & Tobias (2002) have shown that the influence of a surface source in generating dynamo waves is swamped by that of a much weaker α near the tachocline. There are several buoyancy-driven mechanisms that might provide the latter. These include magnetostrophic waves (Moffatt, 1978; Schmitt, 1987), instabilities of flux tubes (Ferriz-Mas, Schmitt & Schüssler, 1994; Ossendrijver, 2000b) and instabilities driven by magnetic buoyancy (Brandenburg & Schmitt, 1998; Thelen, 2000a, b), These last have been studied in considerable detail (see Hughes & Proctor, 1988; Tobias, 2004) in both the linear and nonlinear (Matthews, Hughes & Proctor, 1995; Wissink *et al.*, 2000) regimes, and their interactions with rotational shear have also been explored (Cally, 2000; Hughes & Tobias, 2001; Cline, Brummell & Cattaneo, 2003; Tobias & Hughes, 2004). Another possible source of kinetic helicity arises from MHD instabilities associated with differential rotation within the tachocline, which have been studied and classified (e.g. Gilman & Fox 1999; Cally, 2001, 2003; Gilman & Dikpati, 2002; see Tobias, 2004 for a review).

These instabilities are joint instabilities of the strong toroidal field and latitudinal differential rotation just below the base of the solar convection zone. The global mode associated with the instability is known to possess non-zero kinetic helicity which may be related to the α–effect. However, this connection can only be reliably achieved in a small Rm analysis and for high Rm a straightforward association between kinetic helicity and α–effect is not possible (see Courvoisier, Hughes & Tobias, 2006).

One feature of these instabilities is that they are triggered by a finite-amplitude toroidal field, which itself has to be built up by dynamo action following a supercritical bifurcation; once the buoyancy driven instabilities set in the dynamo can become much more efficient. Thus the branch of nonlinear dynamo solutions may have two turning points, with an intermediate segment of unstable solutions, leading to subcritical behaviour and hysteresis (Ossendrijver, 2000b; *cf.* Figure 3 of Weiss & Tobias, 2000).

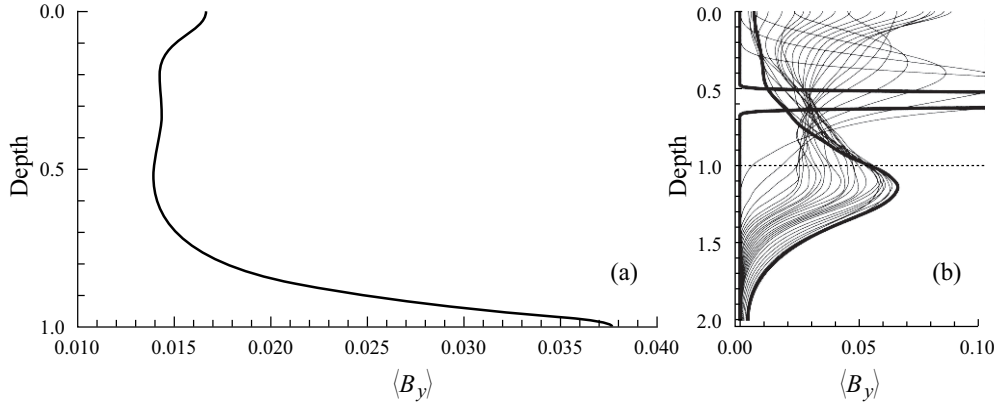

Figure 6.5 - Downward pumping of magnetic flux. Results for a horizontal field, initially in the y–direction and confined to a thin sheet, in a strongly stratified layer. (a) The field $\langle B_y \rangle$, averaged horizontally and over time, as a function of depth in a vigorously convecting layer (courtesy of N.H. Brummell). (b) Evolution with time of $\langle B_y \rangle$ when the convecting layer lies above a layer that is strongly stably stratified; magnetic flux is expelled into the stable region (after Tobias *et al.*, 2001).

6.2.5. MAGNETIC PUMPING

In addition to producing turbulent diffusion and regenerating large-scale fields by the α–effect, turbulent motion can also lead to net transport of magnetic fields. In mean field electrodynamics this is represented by the antisymmetric part of the α–effect ($\alpha^a_{ij} = \varepsilon_{ijk}\gamma_k$). Physically, this corresponds to flux expulsion down the gradient of turbulent intensity and $\boldsymbol{\gamma}$ can be calculated and interpreted as a pumping velocity (Krause & Rädler 1980; Zeldovich, Ruzmaikin & Sokoloff, 1983; Moffatt, 1983). In Boussinesq convection, with up-down symmetry flux is expelled equally towards the top and bottom of the convecting layer. In a stratified layer, however, there is a preferred direction which leads to a net downward transport of magnetic flux. Two distinct mechanisms are involved. For mildly nonlinear convection there are isolated gentle upflows enclosed by a coherent network of downflows and this pattern can give rise to topological pumping (Drobyshevski & Yuferev, 1974). In turbulent convection the sinking network is focused into rapidly descending plumes and this pattern leads to a net downward transport (Weiss, Thomas, Brummell & Tobias, 2004), as illustrated in Figure 6.5a. This process becomes much more effective when there is a stably stratified region beneath the convectively unstable layer as shown in Figure 6.5b (Tobias *et al.*, 1998a, 2001; Dorch & Nordlund 2001). It follows that any large-scale fields within the convection zone will tend to be pumped downwards and into the stably stratified tachocline, where they can accumulate within an even thinner shell that is penetrated by overshooting convection.